Ab initio molecular dynamics calculations of H_2O on BaO(001)

Henrik Grönbeck[1,*] and Itai Panas[2]
[1]*Competence Centre for Catalysis and Department of Applied Physics, Chalmers University of Technology, SE-412 96 Göteborg, Sweden*
[2]*Environmental Inorganic Chemistry, Chalmers University of Technology, SE-412 96 Göteborg, Sweden*
(Received 21 February 2008; revised manuscript received 14 May 2008; published 13 June 2008)

Density functional theory calculations are used to explore water adsorption on BaO(001). The stable configuration is found to be a novel hydroxide pair. A detailed analysis demonstrates that the electrostatic repulsion between the OH^- species is screened by Ba^{2+} cations and that the net interaction is provided by hydrogen bonding. *Ab initio* molecular dynamics at low coverage reveals that the pair is stable at elevated temperatures. The large structural flexibility of the hydoxylated surface may, however, lead to pair dissociation at high coverage. Simulations of a mixed (H_2O+OH) overlayer uncover proton transfer between H_2O and OH groups.

DOI: 10.1103/PhysRevB.77.245419 PACS number(s): 68.43.Bc, 68.47.Gh, 68.43.Pq, 82.65.+r

I. INTRODUCTION

The interaction of water with metal oxide surfaces is fundamental in several areas where heterogeneous catalysis is but one example. Water in molecular or dissociated form may affect catalytic processes both as a promoter[1] and a poison. One example of the latter is its influence on NO_x storage and reduction catalysts where BaO is used as storage material for NO_x.[2] High concentrations of water have been measured to reduce the efficiency of the NO_x uptake.[3] This process is poorly understood and it becomes desirable to unravel the mechanism whereby H_2O interacts with oxide surfaces in general and BaO in particular.

H_2O adsorption on BaO is also interesting from a fundamental point of view as theoretical studies of water adsorption on alkaline earth metal oxides have concerned mainly MgO. *Ab initio* molecular dynamics (AIMD) was earlier applied to compare low coverage H_2O adsorption on MgO(001) and stepped surfaces.[4] Whereas H_2O was found to physisorb on MgO(001), fast dissociation was predicted on stepped surfaces.[4] Subsequent studies at higher H_2O coverage on MgO(001) have discovered a collective dissociation process.[5,6] Here we present a density functional theory (DFT) study of H_2O adsorption on BaO(001). In contrast to MgO(001), water is found to dissociate and form a novel hydroxide (OH^-) pair. The internal electrostatic repulsion of the pair is screened by Ba^{2+} cations and the net attraction is owing to hydrogen bonding. At high coverage, marked structural rearrangements of the oxide surface layer are shown to induce decoupling of the OH^- pairs. Simulations of a mixed (H_2O+OH) overlayer uncover proton transfer between H_2O and OH groups.

Very recently, Carresco and co-workers reported a first-principles study where H_2O dissociation on (001) surfaces of MgO, CaO, and BaO (Ref. 7) was compared. Whereas H_2O remained in molecular state on MgO(001), dissociation into (OH+H) was observed on surfaces with higher basicity. AIMD simulations at 300 K for CaO and BaO indicated that the hydroxide group was trapped to the anion site (O_2^-) where H_2O dissociated. The phenomenon was described as a tight ion pair H_{ads}-OH_{ads}, with an attractive interaction between the subsystems H_{ads} and OH_{ads}. This is an oversimplified description, as will be shown in the present work.

II. COMPUTATIONAL METHOD

The simulations are performed within the pseudopotential plane-wave (PP-PW) implementation of the DFT. In particular, the CPMD code is used.[8–10] The Perdew, Burke and Ernzerhof (PBE) (Ref. 11) formula is used as approximation of the exchange-correlation functional. In a previous report, the performance of different exchange-correlation functionals was investigated on structural and energetic properties of alkaline-earth metal oxide surfaces and PBE was found to provide a good choice.[12] Norm-conserving angular dependent pseudo-potentials are used to describe the interaction between the valence electrons and the atomic cores.[13,14] The one-electron orbitals are expanded in plane waves up to a kinetic energy of 62 Ry. The BaO(001) surface is cleaved from the theoretical bulk lattice (5.59 Å) and modeled with a $p(3\times3)$ slab that consists of three layers. Repeated slabs are separated by 12 Å vacuum. To describe the situation of a BaO surface terminated from a bulk crystal, the bottommost layer is constrained at bulk distance. As the employed super-cell is large, the *k*-point sampling was restricted to the Γ-point. Three layers are sufficient to capture the dynamic properties of H_2O on BaO(001) as verified by a 4 ps simulation at high coverage with a five layer slab. The adsorbate and top-layer surface dynamics is similar in the three and five layer cases. Molecular dynamics is performed with the Car–Parrinello method[8] and a velocity Verlet integrator is used to evolve the equations of motion. Simulations at constant temperature are done by the use of a Nosé–Hoover thermostat. A short time step of 4 au (0.097 fs) is used and the fictitious electron mass is set to 500 au. To enhance the separation between electronic and ionic degrees of freedom, H is replaced with D during the molecular dynamics simulations. Vibrational properties are calculated from the ionic trajectories through the velocity-velocity autocorrelation function or from optimized geometries by use of numerical derivatives.

III. ADSORPTION AT LOW COVERAGE

A. Adsorption dynamics

AIMD is performed for one H_2O molecule in the surface cell, which corresponds to a 1/9 coverage. Initially, the molecule is placed over a cation (Ba^{2+}) site. This represents a

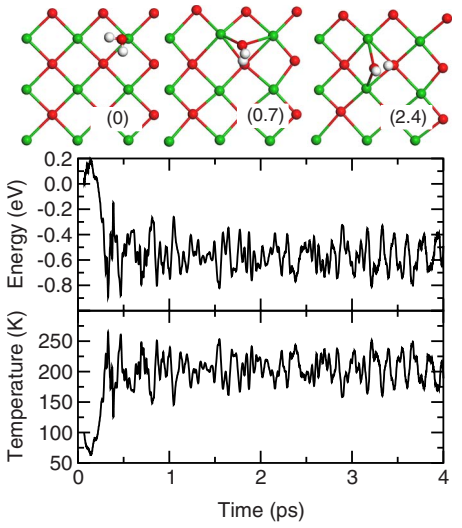

FIG. 1. (Color online) Evolution of Kohn–Sham potential energy (top) and temperature (bottom) during a constant energy molecular dynamics trajectory. The first 4 ps are shown from a 15 ps simulation. The snapshots at 0, 0.7, and 2.5 ps are reported to the right. Atomic color code: Ba (green/gray), oxygen (red/dark), and H (white).

(meta-) stable molecular adsorption site. The system is heated to 100 K during 70 fs and thereafter evolved for ~15 ps in a constant energy trajectory. The potential (Kohn–Sham) energy and temperature for the constant energy part of the simulation is shown together with three snapshots in Fig. 1. The potential energy is reported with respect to the start of the constant-energy part of the simulation. The system overcomes a small energy barrier and reaches an equilibrium energy value of −0.6 eV, which corresponds to a temperature increase of ~100 K. The change in energy and temperature is the result of the rapid dissociation of the H_2O molecule. The snapshots in Fig. 1 show the initial configuration together with two cases of the dissociated product. The water splitting proceeds via a configuration where one H atom in the molecule approaches an oxygen anion in the surface (O_s) and dissociation occurs when the O_s-H-OH angle is close to 180°. Analysis of the charge density during the hydrolysis uncovers the transfer of a proton and the subsequent formation of two hydroxide groups, OH^-_{ads} and $O_sH^-_{ads}$.

A structural analysis of the dissociation process and a part of the subsequent dynamics of the two hydroxide groups is presented in Fig. 2. In Fig. 2(a) the O_s-H_{ads}, $(O\text{-}H)_{ads}$ and

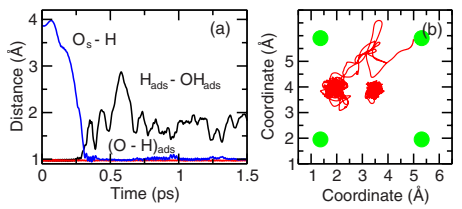

FIG. 2. (Color online) Left: Evolution of interatomic distances during H_2O dissociation on BaO(001). Right: *xy*-projections of the oxygen coordinates in O_sH_{ads} and OH_{ads}. The green/gray filled circles mark the equilibrium positions of neighboring Ba cations.

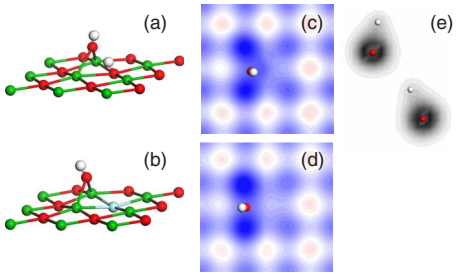

FIG. 3. (Color online) Optimized structures for H_2O (a) and OH (b) adsorbed on BaO(001) and F-BaO(001), respectively. (c) and (d) show the corresponding electrostatic potentials [−5:5] eV ([red/gray:blue/dark gray]) displayed at the position of the O atom in the adsorbed OH group. (e) shows a slice [0.12:1.2] e/au^3 through the charge density of the OH^- pair in (a). The atomic color code as in Fig. 1 with fluorine (blue/dark gray).

H_{ads}-OH_{ads} distances are shown. During dissociation, the O_s-H_{ads} distance is quickly reaching the value of an O-H bond (~1 Å). Simultaneously, the H_{ads}-OH_{ads} distance increases and is fluctuating around 1.7 Å after dissociation. The $(O\text{-}H)_{ads}$ distance is close to 1 Å during the entire trajectory.

Throughout the simulation, OH_{ads} remains close to the site for dissociation. In particular, it visits two different Ba-Ba bridge sites. This is shown in the *xy*-projection of the coordinates for the oxygen atoms in OH_{ads} and O_sH_{ads} [Fig. 2(b)]. See also the snapshots in Fig. 1. Constant temperature simulations at 293 K (6 ps) and 373 K (7 ps) confirm that OH_{ads} is trapped at the O_sH_{ads} site also at higher temperatures.

B. *Analysis of the OH^- pair*

From the molecular dynamics we conclude that H_2O readily dissociates on BaO(001) into a hydroxide pair. Due to the internal electrostatic repulsion, the pairing phenomenon is novel and a detailed analysis of the geometry optimized configuration of the dissociated H_2O molecule has been performed. The analysis comprises structure, vibration frequency, charge, electron density, and electrostatic potential.

1. Analysis of structure and vibration frequency

The optimized geometry is shown in Fig. 3(a). The two O-H distances are calculated to be 0.97 and 1.00 Å for OH_{ads} and O_sH_{ads}, respectively. The O_sH_{ads}-OH_{ads} distance is 1.67 Å. The corresponding OH stretch vibrations are calculated to be 3738 cm^{-1} (OH_{ads}) and 3020 cm^{-1} (O_sH_{ads}). The O-H distance in O_sH_{ads} is slightly longer than an ordinary OH bond and the stretch vibration is red-shifted by ~700 cm^{-1}. These differences are well documented signatures of hydrogen bonded, acid hydroxide groups.[15] A metastable configuration where OH_{ads} is displaced away from O_sH_{ads} is 0.48 eV above the global minimum. In this configuration, the two OH^- groups become equivalent with common O-H distances of 0.97 Å. The stretch vibration is in this case calculated to be 3654 (3707) cm^{-1} for O_sH_{ads} (OH_{ads}).

2. Analysis of charge and electron density

A slice through the electron density of the optimized pair is shown in Fig. 3(e). The density is dominated by O, and the

presence of H is observed as density protrusions. The similarity between the two hydroxide groups is striking, which is in contrast to the description in Ref. 7 of a tight ion H_{ads}-OH_{ads} pair. Due to the dominance of the O density in OH, it is difficult to separate the charge into O and H contributions. Nevertheless, a Mulliken analysis reveals that H is charged by 0.2 and 0.3 for OH_{ads} and O_sH_{ads}, respectively. As the charge on the two species is the same, O_sH_{ads} is only slightly more polarized than OH_{ads}.

3. Analysis of electrostatic potential

In the absence of screening medium, there is a strong electrostatic repulsion between the hydroxide groups. For the di-hydroxide configuration adsorbed on the surface, the gas-phase repulsion is calculated to be 1.7 eV. On the surface, this repulsion is screened by the proximity to Ba^{2+} cations. To exemplify this, the electrostatic potential (ESP) experienced by OH^-_{ads} is shown in Fig. 3(d). The ESP demonstrates the screened repulsion between hydroxides at the $O_sH^-_{ads}$ site. This effect is not owing to polarization of O_sH_{ads}, because isomorphic substitution of O_sH_{ads} by fluorine [F-BaO(001)] produces a very similar ESP; compare 3(c) and 3(d). The optimized structure for OH adsorption at the F-BaO(001) site is shown in Fig. 3(b).

Displacement of OH_{ads} away from the F anion site on F-BaO(001) yields a configuration that is 0.04 eV above the global minimum. This should be compared to 0.48 eV calculated for OH_{ads} attached to O_sH_{ads}. Thus, the trapping of OH_{ads} close to the site for dissociation should be understood as a hydrogen bond. The hydrogen bond in a water dimer is within the present scheme calculated to be 0.22 eV. The polarization of O_sH_{ads} suggests that this bond is stronger in the hydroxide pair.

IV. ADSORPTION AT HIGH COVERAGE

H_2O adsorption on MgO(001) at high coverage is known to be different in nature as compared to low coverage adsorption. Whereas single H_2O on MgO(001) physisorb, collective processes can facilitate dissociation at high coverage.[5,6] Here, the full coverage case is investigated, i.e., one H_2O per BaO surface unit, which for the (3×3) surface cell corresponds to nine molecules.

Initially, the H_2O molecules are placed over Ba^{2+} cations and the trajectory is evolved for 4.6 ps during a constant temperature (293 K) simulation. The initial dynamics of the molecules is similar to the low coverage cases, and four of the nine H_2O molecules dissociate during the first 0.4 ps and form OH^- pairs. At the end of the simulation, six of the nine molecules are dissociated.

As not all molecules find a path to dissociate during the simulation, a mixed (H_2O+OH) overlayer is formed. This overlayer shows interesting proton transfer dynamics. One example is shown in Fig. 4, where snapshots and two representative OH distances are reported. The dissociation of one H_2O molecule has formed an OH^- pair to which a second H_2O molecule is attached (snapshot at 0.43 ps). One of the hydrogen atoms in the H_2O molecule is colored blue/dark. The H_2O-OH_{ads} entity at the O_sH_{ads} site is symmetric with

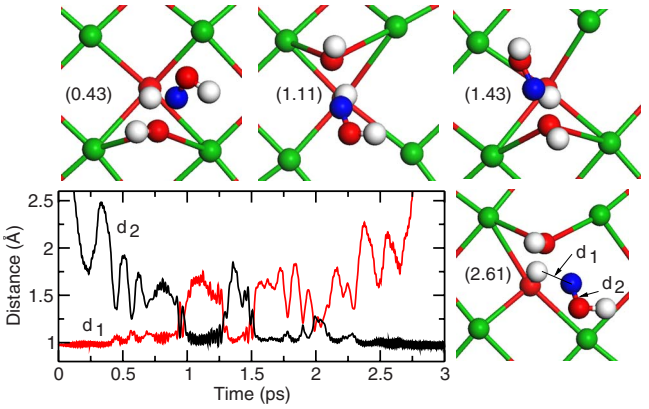

FIG. 4. (Color online) Distances between the blue (dark) hydrogen atom and two oxygen atoms that originate from adsorbed H_2O. The snapshots at 0.43, 1.11, 1.43, and 2.61 ps are shown. The atomic color code as in Fig. 1.

respect to which O atom that should be hydroxide. This situation is manifested by rapid proton transfer from H_2O to OH_{ads}. At 1.11 ps, the blue/dark colored proton in H_2O has been transferred and the d_1 distance has been increased from $\sim$1 Å to $\sim$1.5 Å. Simultaneously, the d_2 distance changes from 1.5 to 1 Å. This kind of proton transfer occurs two more times before an H_2O molecule detaches from the OH^- pair and leaves the site. Note that it is $OH_{ads}H$ that diffuses away from the site and not the H_2O molecule that originally was attached to the OH^- pair.

Another constant temperature (293 K) simulation at unity coverage was evolved with all H_2O molecules initially dissociated and structurally optimized. The full coverage trajectory with dissociated molecules reveals interesting structural dynamics of the oxide. The relaxation and rumpling are shown in the upper left panel of Fig. 5. Relaxation (ρ) refers to the interplane distortion, whereas rumpling (ϵ) measures

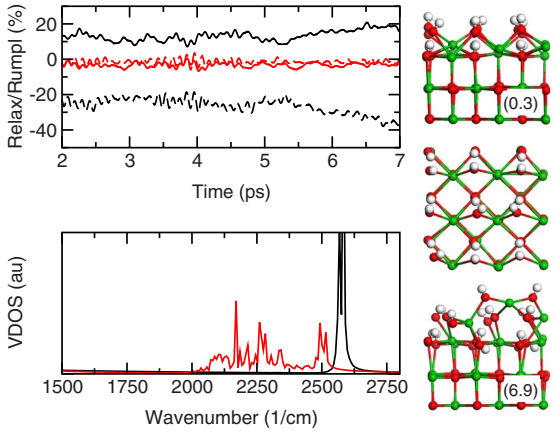

FIG. 5. (Color online) Left upper panel: Relaxation (solid lines) and rumpling (dashed lines) for the first (black) and second (red/gray) surface layer, respectively. Left lower panel: Vibrational density of states. The black and red/gray lines show results for OD_{ads} and O_sD_{ads} groups, respectively. The two snapshots are shown to the right. The upper two models correspond to two views of the structure at 0.3 ps, whereas the lower model represents the structure at 6.9 ps. The atomic color code as in Fig. 1.

the difference in anion and cation displacement:

$$\rho = \frac{d_a + d_c - 2d_b}{2d_b}, \quad (1)$$

$$\epsilon = \frac{d_a - d_c}{d_b}. \quad (2)$$

Here, d_a and d_c are the interlayer distances for the anion and the cation, respectively. d_b is the Ba-O nearest-neighbor distance in the bulk. The OH^- overlayer has a pronounced effect on the surface distortions. For the first surface layer, the relaxation is during the initial 5 ps close to 10% and the rumpling ~−20%. This should be compared with results for the bare surface for which ρ and ϵ are calculated to be −3.6% and −3.0%, respectively. The results for the second surface layer are close to those of the bare surface. After 5 ps, some Ba^{2+} cations are moving out of the surface which further increase the surface distortions. A snapshot from this part of the simulation (6.9 ps) is shown to the right in Fig. 5. As the system turns "disordered," charge screening becomes incomplete which may induce OH^- pair dissociation. Two such cases are shown in Fig. 5. The O_sH_{ads} groups turn around and coordinate via hydrogen bonds toward oxygen anions in the second surface layer.

In the presence of H_2O, there is a thermodynamic preference for BaO to form $Ba(OH)_2$ at the investigated temperature. The formation of $Ba(OH)_2$ requires large structural rearrangements and the configurations in Fig. 5 can be regarded as transient structures in this process. The potential energy of two structures is within the thermal fluctuations (~1 eV) of the system. The adsorption energy per H_2O molecule is 1.31 eV at unity coverage. In fact, the adsorption energy depends weakly on coverage. At 1/9 coverage the adsorption energy for the stable configuration (OH^- pair) is 1.47 eV. These values could be compared with the experimental enthalpy of formation for bulk $Ba(OH)_2$ from BaO and H_2O which is 1.1 eV.[16]

To investigate possible vibrational signatures of OH^- pairs at elevated temperatures and high coverage, a velocity-velocity autocorrelation analysis of the hydrogen (deuterium) trajectories was performed. The result for the high-energy modes is shown in the lower left panel in Fig. 5. The stretch vibration of the OD_{ads} group shows a sharp peak at 2580 cm^{-1}. The corresponding feature for O_sD_{ads} is broad and centered around 2230 cm^{-1}. The large energy spread of this peak is owing to the dynamic coordination of the O_sH_{ads}-OH_{ads} bond in the pairs. If 2580 and 2230 cm^{-1} are scaled by $\sqrt{2}$, we obtain 3650 and 3150 cm^{-1}, respectively. The separation of 500 cm^{-1} is smaller than the shift (700 cm^{-1}) obtained from the static, low coverage case. However, it is pronounced and should be possible to verify experimentally.

V. CONCLUSIONS

To summarize, density functional theory calculations have been used to study H_2O adsorption on BaO(001). AIMD simulations uncover rapid dissociation followed by the formation of a hydroxide pair. Detailed analysis of the pair shows that the electrostatic repulsion is screened by Ba^{2+} cations and that the net O_sH_{ads}-OH_{ads} attraction is provided by hydrogen bonding. Intramolecular hydrogen bonding between hydroxides is well known within, for example, the chemistry of silica surfaces[17] where the pair is stabilized by covalent Si-OH bonds. At low coverage, our simulations show that the hydroxide pair is stable at room temperature for several ps. At high coverage, however, the large structural flexibility of the oxide is found to promote pair dissociation.

ACKNOWLEDGMENTS

Support from the Swedish Research Council and CPU time granted at SNIC is gratefully acknowledged. The Competence Centre for Catalysis is hosted by Chalmers University of Technology and financially supported by the Swedish Energy Agency and the member companies AB Volvo, Volvo Car Corporation, Scania CV AB, GM Powertrain Sweden AB, Haldor Topsoe A/S, and The Swedish Space Corporation.

*Corresponding author: ghj@chalmers.se

[1] A. Bongiorno and U. Landman, Phys. Rev. Lett. **95**, 106102 (2005).
[2] M. Takeuchi and S. Matsomoto, Top. Catal. **28**, 151 (2004).
[3] W. S. Epling, G. C. Campbell, and J. E. Parks, Catal. Lett. **90**, 45 (2003).
[4] W. Langel and M. Parrinello, Phys. Rev. Lett. **73**, 504 (1994).
[5] L. Giordano, J. Goniakowski, and J. Suzanne, Phys. Rev. Lett. **81**, 1271 (1998).
[6] M. Odelius, Phys. Rev. Lett. **82**, 3919 (1999).
[7] J. Carrasco, F. Illas, and N. Lopez, Phys. Rev. Lett. **100**, 016101 (2008).
[8] R. Car and M. Parrinello, Phys. Rev. Lett. **55**, 2471 (1985).
[9] D. Marx and J. Hutter, in *Modern Methods and Algorithms in Quantum Chemistry*, Forschungzentrum Juelich NIC Series Vol. 1 (NIC, FZ Juelich, Germany 2000).
[10] CPMD v3.11.1 Copyright IBM Corp 1990–2001, Copyright MPI fuer Festkoerperforschung Stuttgart 1997–2001.
[11] J. P. Perdew, K. Burke, and M. Ernzerhof, Phys. Rev. Lett. **77**, 3865 (1996).
[12] P. Broqvist, H. Grönbeck, and I. Panas, Surf. Sci. **554**, 262 (2004).
[13] N. Troullier and J. L. Martins, Phys. Rev. B **43**, 1993 (1991).
[14] P. Broqvist, I. Panas, and H. Grönbeck, J. Phys. Chem. B **109**, 9613 (2005).
[15] J. Björnström, A. Martinelli, J. R. T. Johnson, A. Matic, and I. Panas, Chem. Phys. Lett. **380**, 165 (2003).
[16] *Handbook of Chemistry and Physics*, 71st ed, edited by D. R. Lide (CRC, Boca Raton, FL, 1990–1991).
[17] R. K. Iler, *The Chemistry of Silica* (Wiley, New York, 1979), Chap. 6.